Journal of Molecular Catalysis A: Chemical 333 (2010) 85–93

Contents lists available at ScienceDirect

Journal of Molecular Catalysis A: Chemical

journal homepage: www.elsevier.com/locate/molcata

Study of acetaldehyde condensation chemistry over magnesia and zirconia supported on silica

V.V. Ordomsky, V.L. Sushkevich, I.I. Ivanova*

Department of Chemistry, Moscow State University, Lenin Hills, 119892 Moscow, Russia

ARTICLE INFO

Article history:
Received 17 May 2010
Received in revised form 8 September 2010
Accepted 4 October 2010
Available online 30 October 2010

Keywords:
Aldol condensation
Acetaldehyde
IR spectroscopy

ABSTRACT

Aldol condensation of acetaldehyde was investigated over silica supported magnesium and zirconium oxides. The acidic and basic properties of the catalysts were studied by TPD of NH_3 and CO_2 and IR spectroscopy of adsorbed pyridine and CO_2. MgO/SiO_2 catalyst was characterized by high content of both basic and acidic sites, while ZrO_2/SiO_2 contained mainly Lewis acid sites. All materials studied were shown to catalyze the aldol condensation of acetaldehyde with selectivity to crotonaldehyde of ca. 85%. The activity of the catalysts was found to be in the following order: $ZrO_2/SiO_2 > MgO/SiO_2 \gg SiO_2$. To assess the role of acidic and basic sites in condensation reaction, pyridine and carbon dioxide were used as probe molecules for poisoning of the corresponding active sites during catalytic runs. The results pointed to the key role of Lewis acid sites in acetaldehyde condensation. A concerted mechanism involving Lewis and Brønsted acid sites of the catalysts is proposed on the basis of in situ IR spectroscopic studies.

© 2010 Elsevier B.V. All rights reserved.

1. Introduction

Acetaldehyde condensation is among the most important reactions of aldol addition. The significance of this reaction grows nowadays because acetaldehyde can be produced from bioethanol. In the liquid phase, condensation of aldehydes proceeds over both bases or acids [1,2]. However, disadvantages of such processes are well-known: corrosion, separation and environmental problems. Therefore, the development of active and selective heterogeneous catalysts is drawing increasing interest [3–7].

Aldolisation of acetaldehyde has been reported over different heterogeneous catalysts: oxide and mixed oxide systems including MoO_3/SiO_2, WO_3/SiO_2, ZrO_2, ZrO_2–SO_4^{2-} [3], TiO_2, CeO_2, Al_2O_3 [4]; zeolites with MFI [5] and FAU [6] structures, aluminophosphates [7]; hydrotalcite-like materials [8,9], etc. It has been proposed that basic sites of different strength as well as acidic sites of Brønsted and Lewis type can participate in aldol condensation over solid catalysts. However, the detailed information on the role of each type of sites is not always available. Although the mechanisms of the acid- or base-catalyzed aldol condensation in homogeneous catalysis has been proposed and well understood [10,1], this information cannot be easily transferred to heterogeneous catalysis.

Several papers were devoted to the investigation of the mechanism of acetaldehyde condensation over solid catalysts. Biaglow et al. [11] have studied acetaldehyde condensation over acidic zeolite H-ZSM-5. Based on ^{13}C NMR data they proposed the acid-catalysed mechanism of aldol condensation:

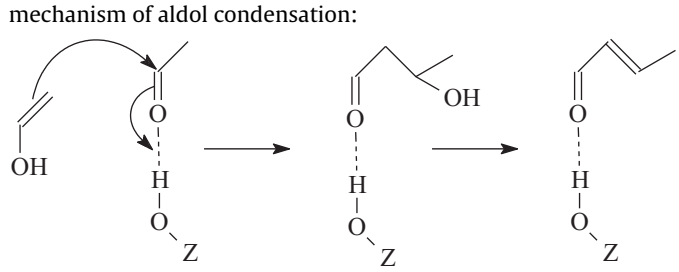

According to this mechanism acetaldehyde is activated on Brønsted acid site of the zeolite to give hydrogen-bonded complex, which interacts with enol form of another acetaldehyde molecule. 3-Hydroxybutanal intermediate formed undergoes further dehydration into crotonaldehyde.

Similar mechanism was proposed by Young and Sheppard [12] for acetaldehyde condensation over silica. The authors believed that the acidity of surface silanol groups is sufficient to promote aldol condensation.

For the other group of catalysts, including calcined layered double hydroxides [7], as well as some oxides such as TiO_2 [13], basic sites were found to play a key role in acetaldehyde self condensation. It has been proposed that basic sites abstract α-proton from the α-carbon position of acetaldehyde to form $^{-}CH_2$–CHO, a nucleophile, which can attack electrofilic carbonyl carbon of another acetaldehyde to form an adsorbed aldol, which upon dehydration produces crotonaldehyde:

* Corresponding author. Fax: +7 495 939 35 70.
E-mail addresses: IIvanova@phys.chem.ru, IIIvanova@phys.chem.msu.ru (I.I. Ivanova).

1381-1169/$ – see front matter © 2010 Elsevier B.V. All rights reserved.
doi:10.1016/j.molcata.2010.10.001

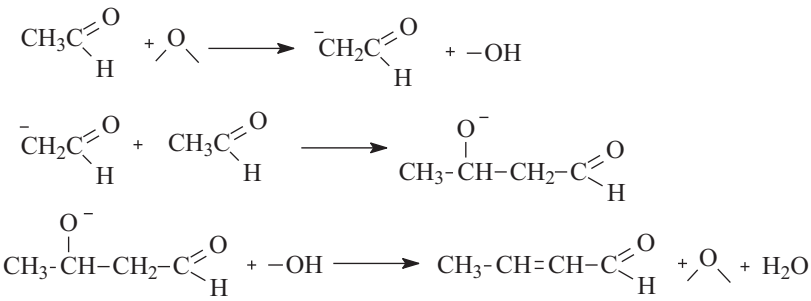

Later on, it has been demonstrated that the aldol condensation over calcined layered double hydroxides require not only basic but also acidic sites. Di Cosimo et al. [14] who studied acetaldehyde condensation over Mg–Al basic oxides proposed bifunctional mechanism of condensation on Lewis acid–strong base pair sites:

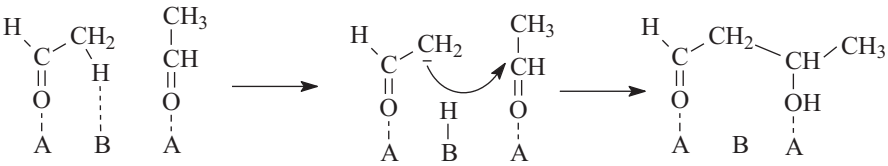

Singh et al. [15] suggested similar mechanism to account for aldol condensation over TiO_2 catalysts:

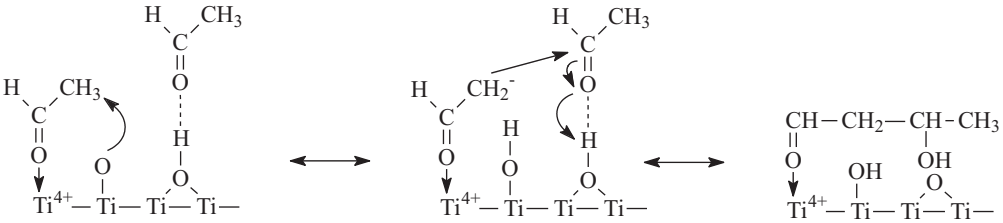

In this mechanism, both Lewis and Brønsted acidic sites are involved. One molecule of aldehyde is attached to Brønsted site via H-bonding, while the another one is adsorbed on Lewis acid site. The mechanism of condensation involves initial abstraction of proton from the α-carbon of acetaldehyde, activated on Lewis acid site by neighboring basic oxygen atom leading to a carbanion formation, which in turn reacts with a second aldehyde molecule activated on Brønsted acid site. 3-Hydroxybutanal intermediate formed undergoes further dehydration into crotonaldehyde [15].

Thus, it appears that the mechanism of condensation strongly depends on the type of the catalyst used. In this work we aimed to clarify the role of acidic and basic sites of different strength in acetaldehyde condensation over MgO/SiO_2 and ZrO_2/SiO_2 catalysts. Pyridine and carbon dioxide were used as probe molecules to study the effect of acidity and basicity.

2. Experimental

2.1. Catalyst preparation

Silica supported catalysts were obtained by incipient wetness impregnation of silica (Silopor 600) with magnesium and zirconium nitrate aqueous solutions. After impregnation all samples were dried at 393 K and calcined at 773 K for 3 h in a flow of dry air. The final catalysts contained 2.0 wt.% of metal oxides. Surface area of the silica-supported catalysts was close to those of the parent Silipor (350 m^2/g).

2.2. Catalyst characterization

Temperature programmed desorption (TPD) of NH_3 and CO_2 was performed in a set-up equipped with TC detector. Prior to NH_3 or CO_2 adsorption, the samples were calcined in a flow of dry air at 823 K for 1 h and, subsequently, in a flow of dry nitrogen for 1 h and cooled down to ambient temperature. The adsorption was carried out for 30 min, in a flow of NH_3 or CO_2 diluted with N_2 (1/1). Subsequently, the physisorbed ammonia or carbon dioxide were removed in a flow of dry He at 373 K for 1 h. Typical TPD experiments were carried out in the temperature range of 295–800 K in a flow of dry He (30 ml/min). The rate of heating was 7 K/min.

IR spectra were recorded on a Nicolet Protégé 380 FT-IR spectrometer at 4 cm^{-1} optical resolution. Prior to the measurements, 20 mg of the catalysts were pressed in self-supporting discs and activated in the IR cell attached to a vacuum line at 723 K for 4 h. The adsorption of pyridine (Py) was performed at 423 K for 30 min. The excess of pyridine was further evacuated at 373 K for 30 min. The adsorption of CO_2 was performed at 298 K for 30 min followed by subsequent evacuation at 298, 373 and 423 K for 10 min. The adsorption of acetaldehyde (crotonaldehyde) was performed at 298 K for 10 min followed by evacuation at 298 K for 10 min. The reaction of acetaldehyde was studied by stepwise increase of the temperature. In a typical experiment, the IR cell was heated up to required temperature, the sample was kept at this temperature for 5 min and cooled down to 298 K for registration of IR spectrum, afterwards the sample was returned to reaction conditions and heated at a further temperature. The reactivity of acetaldehyde was also studied after pre-adsorption of CO_2 or Py.

2.3. Catalytic tests

The catalytic performance was studied in a continuous flow microreactor system. A quartz tube reactor was used. Before the experiment, the catalysts were heated at 773 K in a flow of nitrogen. Then, the temperature was decreased down to the reaction temperature.

Acetaldehyde was fed with saturator which was kept in ice-water bath at 273 K. The reaction was carried out under atmospheric pressure at 403 K. Nitrogen was used as a carrier gas. The

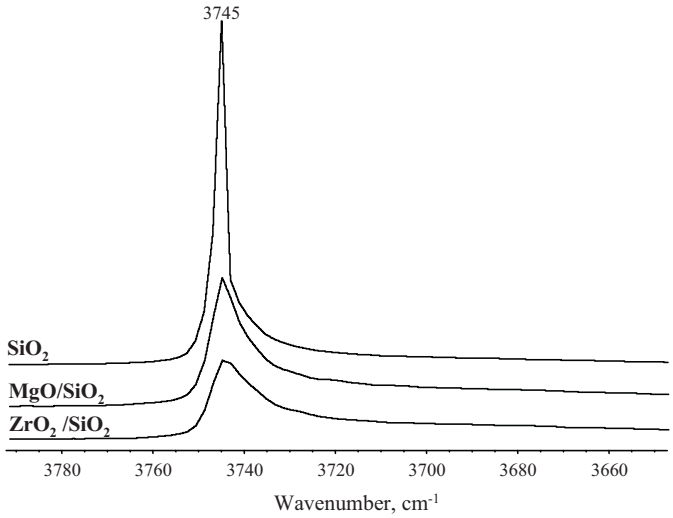

Fig. 1. Infrared spectra of OH-region after evacuation SiO_2, ZrO_2/SiO_2 and MgO/SiO_2.

WHSV of acetaldehyde was within 0.25 or 0.5 g/g h. In some experiments, carbon dioxide or pyridine were co-fed with acetaldehyde with the rate of 2.5 mmol/g h. The products were analyzed online by gas chromatography with 40 m capillary column SE-40. Methane was used as an internal standard. The data were collected after the reaction reached the steady state. The conversion and selectivity were calculated on the carbon mole basis. Selectivity was defined as the total moles of carbon in a product over the total moles of carbon in the sum of products. Initial reaction rates were determined from the initial slope of kinetic curves and defined as a number of moles of acetaldehyde converted into products per hour and per gram of the catalyst.

3. Results and discussion

3.1. Catalyst characterization

The surface OH-groups were studied by IR spectroscopy over the catalysts evacuated at 723 K for 4 h (Fig. 1). The IR spectrum of silica contains an intensive band 3745 cm^{-1} due to isolated surface silanol groups [16]. Deposition of MgO and ZrO_2 over SiO_2 results in significant decrease of the band intensity. In addition, the band becomes broader and shifts to the lower wavenumbers. This result suggests that silanol groups are consumed upon metal oxide deposition due to formation ≡Si–O–M≡ species or strong interaction with dispersed metal oxide particles on the surface [17,18].

The basic properties of the samples were investigated by TPD of CO_2 (Fig. 2). CO_2 TPD curves of ZrO_2/SiO_2 and SiO_2 do not show any significant difference except high temperature peak at 700 K observed for ZrO_2/SiO_2. The situation is different for MgO/SiO_2 for which the peak at about 373 K corresponding to weak basic sites is much more intensive. These data are in line with the results published previously for supported magnesia and zirconia [19,20]. Supported MgO and ZrO_2 display different basic properties in comparison with bulk oxides. The high temperature component which was observed in the case of bulk oxides is significantly smaller for supported oxides because of the strong interaction between deposited oxides and silica [17,18]. Bulk MgO exhibits stronger basic properties in comparison with ZrO_2. This accounts for higher content of basic sites in supported MgO system.

FTIR spectra of adsorbed CO_2 confirm the above data (Fig. 3). While in the case of MgO/SiO_2 intensive bands in the region of 1700–1400 cm^{-1} are observed due to CO_2 adsorption on basic sites, only weak bands are detected over ZrO_2/SiO_2. According

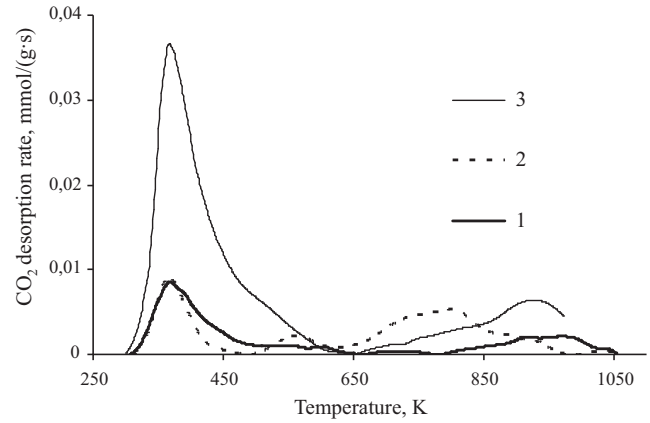

Fig. 2. CO_2 TPD profiles over parent SiO_2 (1), ZrO_2/SiO_2 (2) and MgO/SiO_2 (3).

to the literature data [21–23] the IR bands can be assigned to three types of surface species: bicarbonate, unidentate and bidentate carbonate. A symmetric and an asymmetric O–C–O stretching vibrations at 1673 and 1440 cm^{-1} indicates bicarbonate species formation over MgO/SiO_2 [24,25]. Bicarbonate species over ZrO_2/SiO_2 became apparent by small intensive shoulder at 1630 and band at 1440 cm^{-1} [26]. Bicarbonate species are weakly adsorbed on basic OH-groups and disappear after heating to 373 K (Figs. 2 and 3). The band at 1615 cm^{-1} can be attributed to O–C–O stretching vibration in bidentate carbonate formed on Lewis acid–Brønsted base pairs of MgO/SiO_2 [27]. For the ZrO_2/SiO_2 sample, the main band at 1600 cm^{-1} due to bidentate carbonate is observed [26]. This form of adsorped CO_2 is stable in contrast to bicarbonate species and desorbs only at 423 K (Fig. 3). Unidentate carbonate is the main adsorption state of CO_2 on bulk MgO and ZrO_2 [25,26] but not typical for supported oxides over SiO_2 [17,19]. Thus, the adsorption of CO_2 revealed several types of basic sites on MgO/SiO_2 catalyst: medium basic sites in Lewis acid–base pairs in –Mg–O– species incorporated in silica and weak basic OH-groups.

Acidic properties of MgO/SiO_2, ZrO_2/SiO_2 and SiO_2 samples were investigated by TPD of NH_3. The results are presented in Fig. 4.

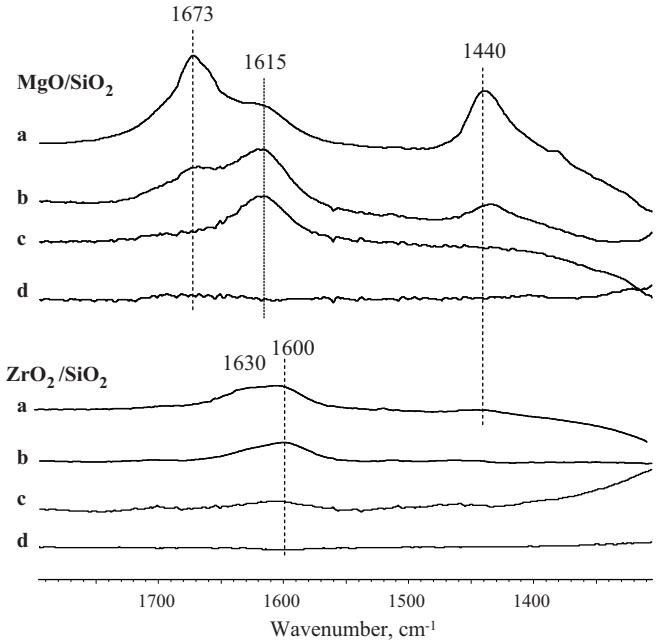

Fig. 3. FTIR spectra observed after adsorption of CO_2 over ZrO_2/SiO_2 and MgO/SiO_2 (a) and evacuation at 298 K (b), 373 K (c) and 423 K (d).

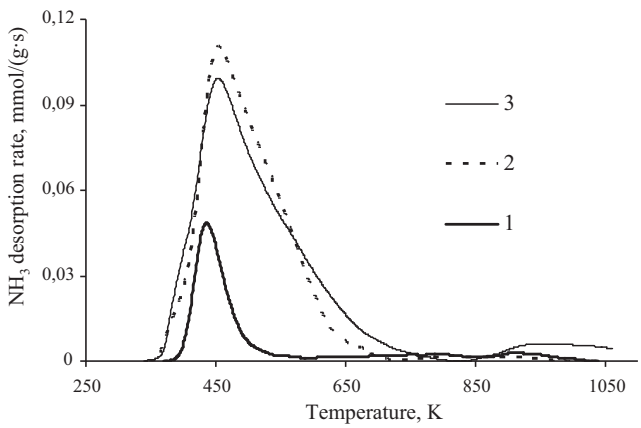

Fig. 4. NH_3 TPD profiles over SiO_2 (1), ZrO_2/SiO_2 (2) and MgO/SiO_2 (3).

Table 1
Content of basic and acid sites.

Catalyst	Amount of sites	
	Basic (μmol/g)[a]	Acidic (μmol/g)[b]
MgO/SiO_2	37.4	116.0
ZrO_2/SiO_2	13.5	118.0
SiO_2	8.4	29.7

[a] Determined by TPD CO_2.
[b] Determined by TPD NH_3.

The quantitative data on the amount of sites are given in Table 1. NH_3 TPD profiles on MgO/SiO_2 and ZrO_2/SiO_2 show the only intensive peak at about 470 K and suggest that the samples have only weak acid sites. The amount of NH_3 desorbed is much higher on supported oxides than on parent SiO_2 (Table 1).

The nature of acid sites was examined by IR spectroscopy of adsorbed pyridine (Fig. 5). The infrared spectra of pyridine adsorbed on metal oxides show the characteristic IR bands in the spectral region of 1700 and 1300 cm^{-1}. The main bands observed at 1595 and 1446 cm^{-1} are due to H-bonded pyridine [28,29]. These bands are the only bands observed in the case of silica (Fig. 5). The band at 1540 cm^{-1} corresponding to protonated pyridine was not observed on the samples studied. The result suggests that pure SiO_2 has neither Lewis nor Brönsted acid sites capable to interact with gaseous pyridine.

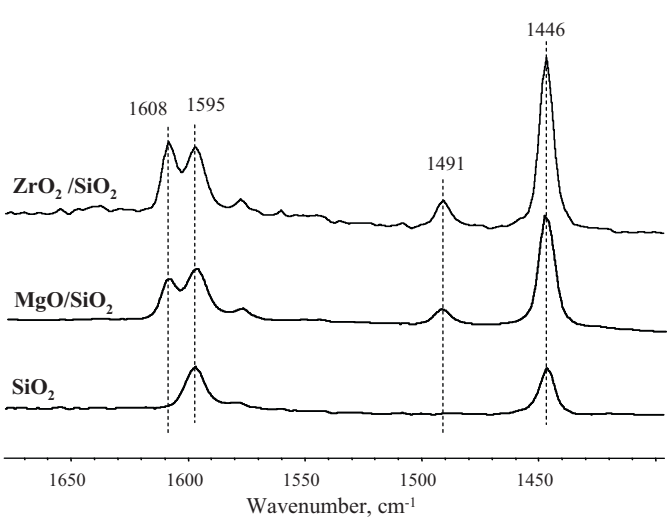

Fig. 5. FTIR spectra observed after adsorption of pyridine over SiO_2, ZrO_2/SiO_2 and MgO/SiO_2 catalysts.

On the contrary, ZrO_2/SiO_2 and MgO/SiO_2 reveal distinct bands at 1608, 1491 and more intensive band at 1446 cm^{-1}. These bands are due to pyridine adsorbed on the Lewis acid sites. The formation of Lewis acid sites over ZrO_2/SiO_2 may result from dehydroxylation of zirconia during calcination procedure [30]. Lewis acidity of the MgO/SiO_2 can be due to low-coordinated atoms of magnesium on the edges and sides of MgO crystallites [31,32].

Consequently, the investigation of the acid–base properties of supported oxides pointed that MgO/SiO_2 contains higher number of basic sites in comparison with ZrO_2/SiO_2, while the amount of Lewis acid sites is comparable on both samples.

3.2. Catalytic results

The catalytic activity of the catalysts in acetaldehyde condensation was characterized by initial rates of acetaldehyde conversion. The initial rates determined at 403 K were found to be 0.63 μmol/g s for ZrO_2/SiO_2, 0.45 μmol/g s for MgO/SiO_2 and 0.015 μmol/g s for SiO_2. Thus, ZrO_2/SiO_2 and MgO/SiO_2 demonstrated rather high activity with respect to pure SiO_2. Silica was practically inactive in aldol condensation. It is interesting to note that the activity of supported catalysts does not correlate with the basicity of the samples. Although MgO/SiO_2 exhibits much higher number of basic sites (Table 1) its activity was found to be lower.

The data on the selectivity towards crotonaldehyde and other by-products obtained over ZrO_2/SiO_2 and MgO/SiO_2 catalysts are presented in Table 2 for the same conversion levels of acetaldehyde.

The results show that the selectivity to crotonaldehyde over the systems studied was within 83–87%. The main by-products included acetone, methyl vinyl ketone, ethyl acetate, 2,4-dimethyl-1,3-dioxane and 2,4-hexadienal. The formation of all products detected can be described by the reaction pathways shown in Fig. 6. Condensation of acetaldehyde leads to 3-hydroxybutanal which is dehydrated into crotonaldehyde [33]. 3-Hydroxybutanal is not present in the products which is in line with the results of other authors [3]. This product is very unstable at our reaction conditions and undergoes fast dehydration. Crotonaldehyde may further interact with another molecule of acetaldehyde with formation of 2,4-hexadienal [7]. 2,4-Dimethyl-1,3-dioxane can be formed from crotylalcohol and acetaldehyde via a pathway similar to those reported in [34] for condensation of isobutylene and formaldehyde into 4,4-dimethyl-1,3-dioxane. 3-Hydroxybutanal (enolate) can be also converted to the keto form via intramolecular H transfer [35]. 4-Hydroxybutan-2-al formed can be further transferred into methyl vinyl ketone via dehydration or into acetone and formaldehyde via reverse reaction to aldol condensation [36]. Acetaldehyde can be also oxidized by surface oxygen as it was previously observed on several oxides such as ZnO, TiO_2 and CeO_2 [36,37]. The reaction of acetic acid with alcohols leads to formation of acetates.

Selectivity of acetaldehyde conversion into crotonaldehyde is slightly higher on MgO/SiO_2 with respect to ZrO_2/SiO_2. The main by-products observed over MgO/SiO_2 are mostly due to acetaldehyde polycondensation. On the contrary, in the case of ZrO_2/SiO_2 quite high contents of acetone, methyl vinyl ketone and ethyl acetate are observed. This observation could be due to the presence of redox sites over zirconium dioxide along with acidic and basic sites [38].

To elucidate the nature of the active sites, acidic or basic probe molecules were added to the feed in order to poison corresponding active sites. The results are summarized in Fig. 7. On the contrary, co-feeding of carbon dioxide which is supposed to be adsorbed on the basic sites has no effect on the catalytic activity of both magnesium and zirconium oxides supported on silica. Co-feeding of pyridine results in significant decrease of the activity over both supported catalysts. Dramatic inhibition of activity by addition of

Table 2
Selectivity to the products of acetaldehyde transformation over MgO/SiO_2 and ZrO_2/SiO_2 catalysts at the same conversion level.

Catalyst	WHSV (g/g h)	Conversion (%)	Selectivities (carbon atom – %)					
			Crotonaldehyde	Acetone	Methyl vinyl ketone	Ethyl acetate	2,4-Dimethyl-1,3-dioxane	2,4-hexadienal
MgO/SiO_2	0.25	30.6	87.6	0.7	–	–	3.6	8.0
ZrO_2/SiO_2	0.5	28.3	83.4	5.6	6.2	0.19	3.9	0.7

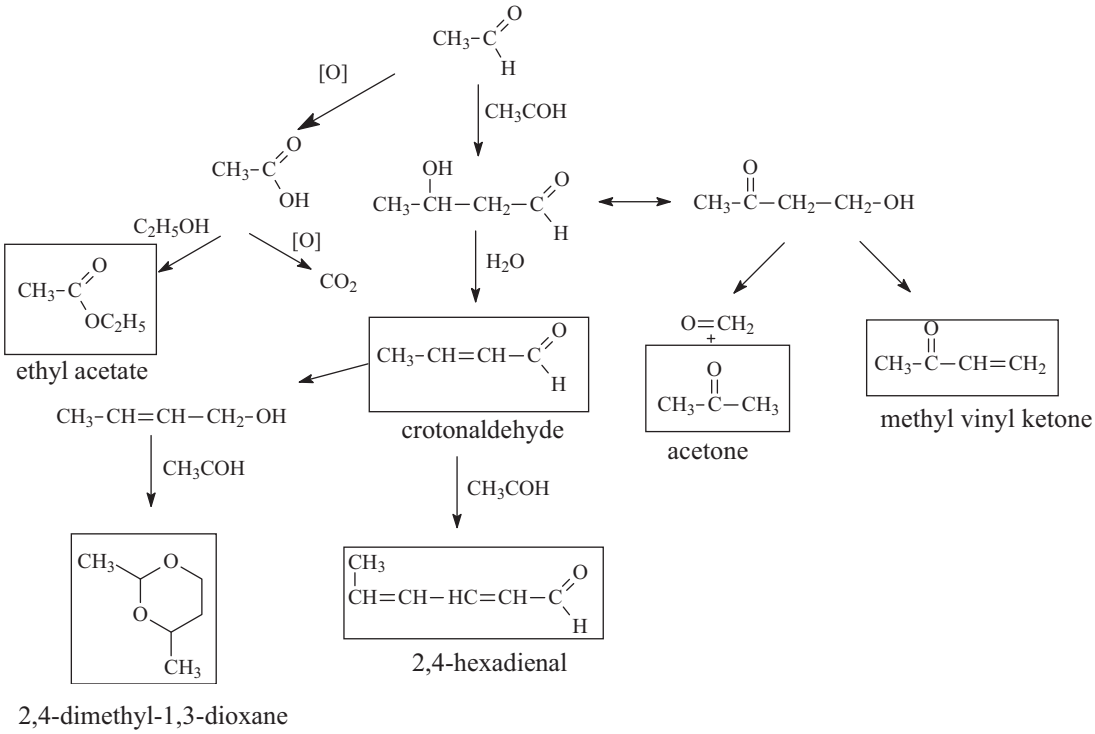

Fig. 6. Reaction scheme for acetaldehyde conversion on MgO/SiO_2 and ZrO_2/SiO_2.

pyridine suggests that Lewis acid sites play important role in the aldol condensation of acetaldehyde.

The results obtained are in contradiction with the results published by Zhang et al. [39], who observed higher activity of bulk MgO with respect to ZrO_2 in condensation of butyraldehyde. Pre-adsorption of CO_2 showed significant decrease of the activity of MgO but NH_3 had no effect. This contradiction can be accounted for by different mechanisms of butyraldehyde and acetaldehyde activation. Abstraction of proton from the secondary carbon atom in butyraldehyde should proceed easier on basic site than in the case of primary carbon in acetaldehyde:

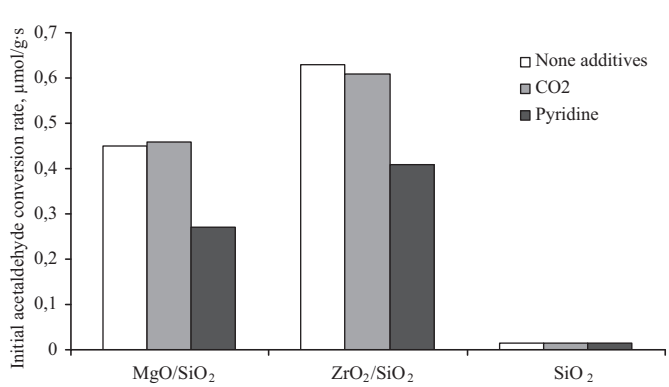

Fig. 7. Initial rates of acetaldehyde conversion in the absence and in the presence of CO_2 and pyridine.

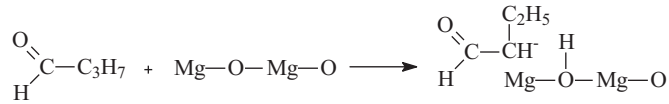

It can be proposed that in the case of acetaldehyde the preliminary activation on Lewis site leading to an increase of the positive charge of carbon in carbonyl group is required:

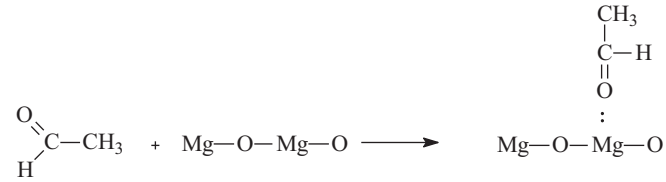

This hypothesis can be confirmed by IR spectroscopic study of acetaldehyde reaction in the presence of probe molecules.

3.3. FTIR study of acetaldehyde transformations

The IR spectra recorded after adsorption of acetaldehyde on ZrO_2/SiO_2, MgO/SiO_2 and SiO_2 are compared in Fig. 8.

The exposure of SiO_2 to 1.3 kPa of acetaldehyde results in appearance of the bands similar to those of gas-phase acetaldehyde (Fig. 8a): 3003 cm^{-1} ($\nu_{as}(CH_3)$), 2926 cm^{-1} ($\nu_s(CH_3)$), 2857 cm^{-1} ($2\nu_6A'$ Fermi), 2767 cm^{-1} ($\nu(CH)_{ald}$), 1725 cm^{-1} ($\nu(C{=}O)$, 1430 cm^{-1} ($\delta_{as}(CH_3)$), 1400 cm^{-1} ($\delta_s(CH_3)$) and 1355 cm^{-1} ($\delta_s(CH)$) [15]. The subsequent evacuation of the sample allows

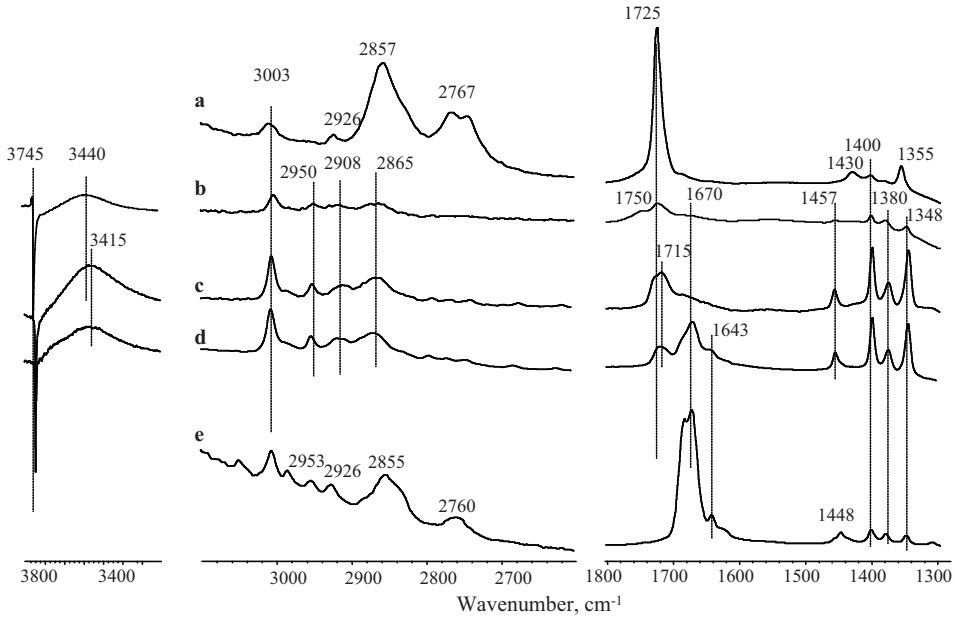

Fig. 8. Infrared spectra obtained after exposure of SiO_2 to 1.3 kPa of acetaldehyde (a), 1.3 kPa of crotonaldehyde (e) and after exposure of SiO_2 (b), ZrO_2/SiO_2 (c) and MgO/SiO_2 (d) to 1.3 kPa of acetaldehyde with subsequent evacuation at 298 K.

observation of strongly adsorbed acetaldehyde species (Fig. 8b). Hill et al. [40] identified two types of species persisting on silica: physisorbed acetaldehyde and oligomeric acetaldehyde such as paraldehyde or metaldehyde. The bands observed at ca. 2865, 1725 and 1348 cm^{-1} could be assigned to the former, while the bands at 3003, 2950 and 1400 cm^{-1} are probably due to the latter.

The appearance of the broad band at 3440 cm^{-1} which is accompanied by the decrease of the intensity of ν(O–H) band of silanol groups at 3745 cm^{-1} (Fig. 8b) is indicative of the interaction of silanol groups with acetaldehyde and points to acetaldehyde adsorption onto silica via H-bonding (≡Si–O–H···O=C⟨). Strong H-bonding with weakly acidic silanol groups of silica could be induced by the adsorption of the second acetaldehyde molecule on the neighboring oxygen atom:

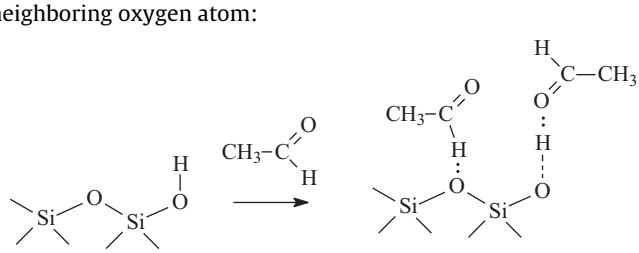

The effect of induced acidity of silanol groups by coadsorption of different molecules was described earlier by Tsyganenko et al. [41].

Besides the bands which can be attributed to acetaldehyde adsorption, two weak lines are detected at 1750 and 1670 cm^{-1}. While the band at 1750 cm^{-1} could be attributed to carbonyl stretching vibration in silyl acetate [42], the band at 1670 cm^{-1} points to formation of small amounts of crotonaldehyde or 3-hydroxybutanal on the surface of the silica already at ambient temperature. The position of the latter band was confirmed in a separate experiment on crotonaldehyde adsorption over silica (Fig. 8e), Young and Sheppard [12] suggested that aldol condensation of acetaldehyde proceeds via acidic mechanism initiated by surface hydroxyl groups of silica:

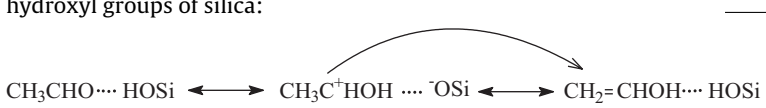

The adsorption of acetaldehyde on ZrO_2/SiO_2 leads to a different picture (Fig. 8c). First of all, the intensity of all bands of acetaldehyde is much higher due to the stronger adsorption of acetaldehyde over this catalyst. Secondly, the band at 3440 cm^{-1} shifts to lower wavenumbers and increases in intensity pointing to the stronger H-bonding of acetaldehyde to silanol groups over this catalyst. Actually, the increase of the acidity of silanol groups after incorporation of zirconia by impregnation procedure was discussed earlier by Baigrie et al. [2]. Finally, the band corresponding to ν(C=O) of acetaldehyde (1715 cm^{-1}) is shifted with respect to the ν(C=O) band in the gas phase spectrum (Fig. 8a) and in the spectrum of acetaldehyde adsorbed on SiO_2 (Fig. 8b). This result suggests that on ZrO_2/SiO_2, acetaldehyde is adsorbed not only via H-bonding to silanol groups (≡Si–O–H···O=C⟨) but also via strong interaction of the carbonyl group with Lewis sites, most probably coordination-unsaturated Zr^{4+} (⟩C=O Zr^{4+}).

The intensity of the band at 1670 cm^{-1} corresponding to ν(C=O) in crotonaldehyde or 3-hydroxybutanal is higher in the case ZrO_2/SiO_2 than on silica, which is in line with higher activity of this catalyst in aldol condensation (Fig. 8).

The IR spectrum of acetaldehyde adsorbed over MgO/SiO_2 (Fig. 8d) is similar to those observed over ZrO_2/SiO_2. The major difference is in increase of the contribution of the band at 1670 cm^{-1} and the appearance of the band at 1643 cm^{-1} due to ν(C=C) mode of crotonaldehyde. This result suggests that MgO/SiO_2 catalyst should be more active in condensation than ZrO_2/SiO_2 which is however in contradiction with the catalytic data presented in Fig. 7 and will be discussed in more detail latter.

The IR spectra of acetaldehyde conversion at elevated temperatures over the catalysts studied are shown in Figs. 9–11. In the case of silica, heating of the sample to 373 K and 453 K leads to gradual decrease of the bands attributed to all forms of adsorbed acetaldehyde (Fig. 9). At the same time, the intensity of the band at 1670 cm^{-1} attributed to ν(C=O) in crotonaldehyde or 3-hydroxybutanal increases. The band at 1640 cm^{-1} due to ν(C=C) of crotonaldehyde is not observed in the spectra either due to

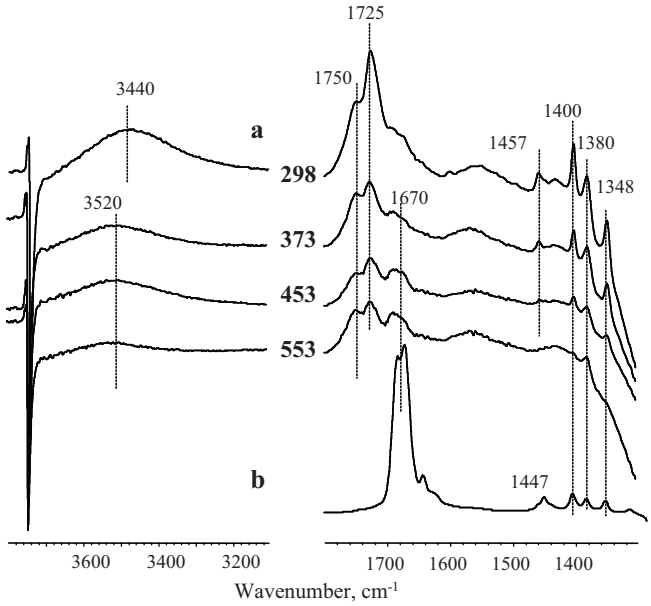

Fig. 9. Infrared spectra obtained after acetaldehyde adsorption and reaction over SiO_2 (a) and after adsorption of crotonaldehyde over SiO_2 (b).

the low intensity, or due to the limitations in dehydration of 3-hydroxybutanal into crotonaldehyde over silica. Condensation of acetaldehyde at elevated temperatures is accompanied by the shift of the band at 3440 cm^{-1} to higher wavenumbers and by the decrease of its intensity, which points to weaker H-bonding of 3-hydroxybutanal or crotonaldehyde to silica.

Strong interaction of acetaldehyde with OH-groups of silica and partial release of the silanol groups in the course of acetaldehyde transformation into crotonaldehyde points to the participation of silanol groups in the condensation reaction as it was proposed earlier by Young and Sheppard [12]. We believe however that concerted mechanism presented below will better account for high reactivity of weakly acidic ≡SiOH group and for our IR results:

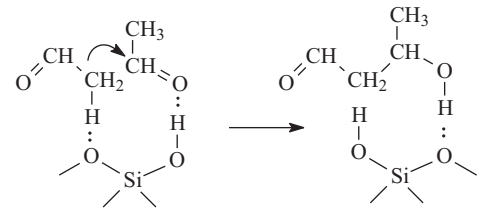

The results on acetaldehyde conversion over ZrO_2/SiO_2 sample are presented in Fig. 10. Heating the sample to 373 K results in almost complete transformation of acetaldehyde into crotonaldehyde as evidenced by rapid decrease of the band at 1715 cm^{-1} (ν(C=O) of acetaldehyde) followed by the increase of the bands at 1670 cm^{-1} and 1643 cm^{-1} due to ν(C=O) and ν(C=C) in crotonaldehyde [12,15]. Transformation of acetaldehyde into crotonaldehyde is accompanied by the decrease of the band due to hydrogen-bonded silanol groups as well as the intensities of the bands in the region of 1460–1340 cm^{-1} due to C–H vibrations. These observations can be explained by weaker interaction of crotonaldehyde with ZrO_2/SiO_2 surface sites and therefore lower polarization of C–H bonds [43]. Further heating to 453 K doesn't result in any changes in the spectra.

To investigate the role of the acidic and basic sites of ZrO_2/SiO_2 in aldol condensation, acetaldehyde was reacted on the samples with pre-adsorbed pyridine or CO_2. The background spectra of adsorbed pyridine and CO_2 were subtracted from the spectra with adsorbed acetaldehyde. The IR spectra are presented in Fig. 10b and c. CO_2 pre-adsorption does not lead to any significant changes in spectral features. On the contrary, pyridine pre-adsorption results in dramatic decrease of the bands corresponding to acetaldehyde and in the inhibition of crotonaldehyde formation in all the temperature range. Consequently, poisoning of Lewis acid sites by pyridine prevents both the adsorption and aldolization of acetaldehyde. Thus, our IR results confirmed that Lewis acid sites participate in acetaldehyde condensation over ZrO_2/SiO_2 catalyst along with acidic silanol groups and suggested that the enhanced activity of this catalyst with respect to silica is due to the presence of Lewis sites.

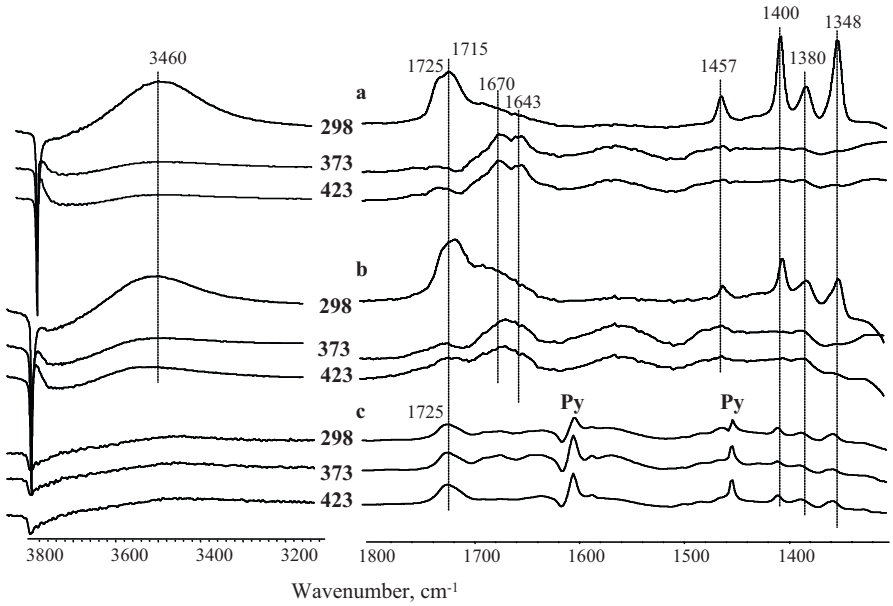

Fig. 10. Infrared spectra obtained after acetaldehyde adsorption and reaction over fresh ZrO_2/SiO_2 (a), over ZrO_2/SiO_2 with pre-adsorbed CO_2 (b) and over ZrO_2/SiO_2 with pre-adsorbed pyridine (c).

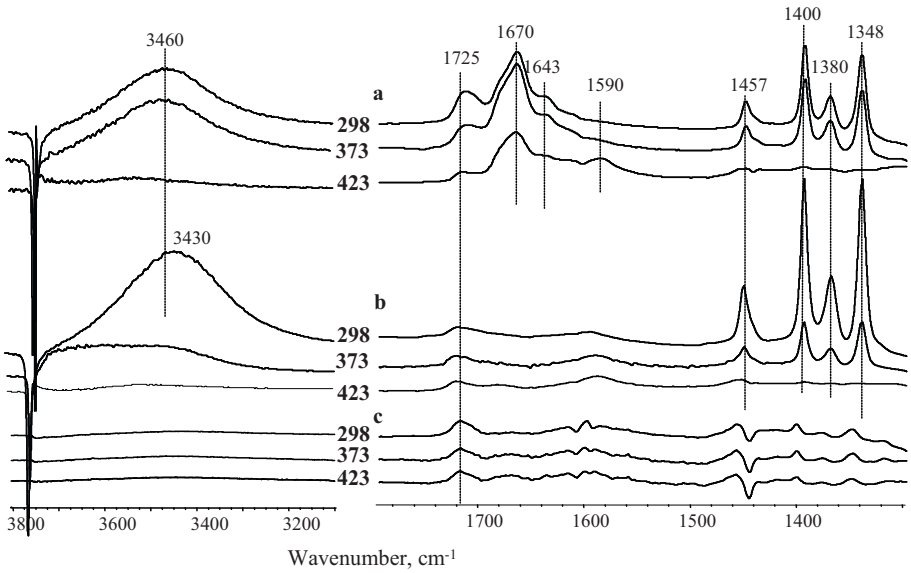

Fig. 11. Infrared spectra obtained after acetaldehyde adsorption and reaction over fresh MgO/SiO_2 (a), over MgO/SiO_2 with pre-adsorbed CO_2 (b) and over MgO/SiO_2 with pre-adsorbed pyridine (c).

To account for all the above observations, the following mechanism of acetaldehyde condensation was proposed for ZrO_2/SiO_2 catalyst:

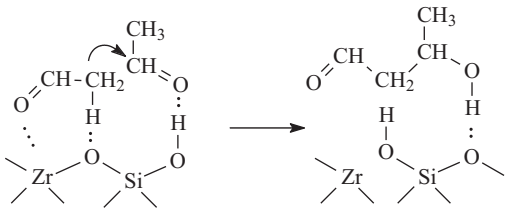

According to this mechanism, incorporation of zirconia in silica results in formation of Lewis acid sites and induces Brønsted acidity of silanol groups [44,45]. Acetaldehyde molecules absorb on both sites. Due to the interaction of carbonyl group with coordination-unsaturated Zr atom, the basicity of the neighboring oxygen increases, which favors the abstraction of proton from the methyl group of the first acetaldehyde molecule and its interaction with the second acetaldehyde molecule protonated on the silanol group. As a result, 3-hydroxybutanal is formed and the active sites of the catalyst are regenerated. Further dehydration of 3-hydroxybutanal into crotonaldehyde occurs most probably on the Lewis acid sites of the catalyst. The higher reactivity of ZrO_2/SiO_2 catalyst with respect to silica is due to the presence of the Lewis sites which enhance the basicity of the neighboring oxygen and induce acidity of the silanol group.

The mechanism proposed for acetaldehyde condensation over ZrO_2/SiO_2 is similar to those suggested previously by Singh et al. [15] for aldol condensation on Lewis acid–base pairs and Brønsted acid sites of TiO_2. The role of Lewis acid–base pairs and Brønsted sites in our case is provided by ≡Zr–O-pairs incorporated in silica and acidic silanol groups with induced acidity, respectively.

The IR spectra obtained over MgO/SiO_2 are shown in Fig. 11. As it was mentioned above transformation of acetaldehyde into crotonaldehyde on this catalyst occurs to a considerable extent already at ambient temperature. However, further transformations lead to the diminishing of the reaction rate. While on ZrO_2/SiO_2 catalyst, all acetaldehyde is converted at 373 K (Fig. 10a), on MgO/SiO_2 complete conversion is not achieved even at 453 K (Fig. 11a). This result suggests that rapid reaction takes place only on fresh catalyst, while at longer reaction times the strong active sites are poisoned by reactants or products and the reaction proceeds on weaker sites. Poisoning of the strong sites could be due to acetaldehyde polycondensation confirmed by the appearance of the band at 1590 cm^{-1} which can be attributed to C=O stretching vibrations in 2,4-hexadienal. This observation is in line with catalytic data presented in Table 2.

It is proposed that on fresh MgO/SiO_2 catalyst acetaldehyde reacts over strong basic sites via reaction pathway similar to those proposed by Kagunya and Jones [7] or Di Cosimo et al. [14]:

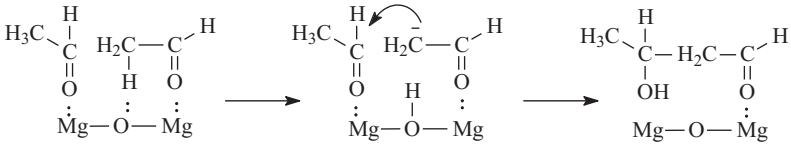

The existence of strong basic sites over MgO/SiO_2 such as isolated surface O^{2-} ions has been confirmed by IR spectroscopy of adsorbed CO_2 (Fig. 3). The appearance of such sites could be due to formation of magnesia islands over the silica surface [19]. To confirm the participation of strong basic sites in the initial steps of the reaction over MgO/SiO_2 the experiment over the catalyst with pre-adsorbed CO_2 was carried out (Fig. 11b). The following differences image:

- the bands due to crotonaldehyde formation do not appear;
- the intensities of the bands in the region of ν(C=O) vibrations of acetaldehyde decrease, while of the intensities of the bands in the region of C–H vibrations increase;
- the band corresponding to hydrogen-bonded complex with silanol groups increases in intensity and shifts to the lower wavenumbers.

The prevention of crotonaldehyde formation could be explained by poisoning of the strong basic sites such as O^{2-} ions in MgO islands responsible for rapid acetaldehyde condensation over fresh

catalyst, while strong H-bonding of acetaldehyde to silanol groups can be induced by interaction of CO_2 with –Mg–O–Si–OH sites:

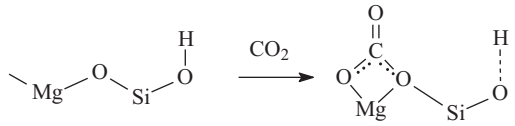

The results obtained suggest that strong basic sites existing over MgO/SiO_2 are more reactive in condensation than acidic sites of ZrO_2/SiO_2. However they are quickly deactivated and further reaction proceeds over Lewis acid–weak base –Mg–O-pairs and Brønsted acidic sites via the mechanism similar to those proposed for ZrO_2/SiO_2 catalyst. To check this, the experiment with pre-adsorbed pyridine was carried out. As in the case of ZrO_2/SiO_2 catalyst, pre-adsorption of pyridine results in almost complete disappearance of the bands of acetaldehyde and crotonaldehyde over MgO/SiO_2 (Fig. 11c), confirming that second reaction pathway may play an important role over MgO/SiO_2.

Thus, the IR study pointed to two mechanistic pathways of acetaldehyde condensation which may take place over MgO/SiO_2: (i) basic reaction mechanism including intermediate carbanion formation over strong basic sites and (ii) concerted mechanism involving Lewis acid–weak base –Mg–O-ion pairs and silanol groups with induced acidity.

The latter reaction pathway most probably governs the conversion of acetaldehyde over MgO/SiO_2 and ZrO_2/SiO_2 under real conditions and accounts for the catalysts reactivity sequence observed during catalytic runs in the presence and in the absence of pyridine and CO_2 (Fig. 7).

4. Conclusions

It has been demonstrated that over ZrO_2/SiO_2 catalyst the acetaldehyde condensation proceeds over Lewis acid–weak base ≡Zr–O-pairs and Brønsted acid sites represented by silanol groups with induced acidity. The concerted mechanism proposed involves activation of acetaldehyde molecule on ≡Zr–O-pair, abstraction of proton from its methyl group and formation of C–C bond between the methylene group formed and methylene group of the second acetaldehyde molecule protonated on the Brønsted acid site. 3-Hydroxybutanal undergoes further dehydration into crotonaldehyde.

Over MgO/SiO_2, two mechanistic pathways of acetaldehyde condensation were identified: (i) basic reaction pathway over strong basic sites most probably represented by O^{2-} ions in MgO islands on silica surface; and (ii) concerted mechanism similar to those proposed for ZrO_2/SiO_2 and involving Lewis acid–weak base –Mg–O-pairs incorporated in silica and silanol groups with induced acidity.

The IR spectroscopic results suggest that strong basic sites existing over MgO/SiO_2 are more reactive in condensation than Lewis and Brønsted acidic sites of both ZrO_2/SiO_2 and MgO/SiO_2. However, these sites are quickly deactivated. Therefore, the reaction pathway involving Lewis acid–weak base pairs and Brønsted acid sites most probably governs the conversion of acetaldehyde over MgO/SiO_2 and ZrO_2/SiO_2 under real conditions. This reaction pathway accounts for the catalyst reactivity sequence observed during catalytic runs: $ZrO_2/SiO_2 > MgO/SiO_2 \gg SiO_2$ and explains the key role of Lewis acidic sites in aldol condensation over magnesium and zirconium supported catalysts.

References

[1] R.N. Hayes, R.P. Grese, M.L. Gross, J. Am. Chem. Soc. 111 (1989) 8336.
[2] L.M. Baigrie, R.A. Cox, H.S. Tilk, M. Tencer, T.T. Tidwell, J. Am. Chem. Soc. 107 (1985) 3640.
[3] W. Ji, Y. Chen, H.H. Kung, Appl. Catal. A 161 (1997) 93.
[4] J. Rasko, J. Kiss, Appl. Catal. A: Gen. 287 (2005) 252.
[5] E. Dumitriu, V. Hulea, I. Fechete, A. Auroux, J. Lacaze, C. Guimon, Micropor. Mesopor. Mater. 43 (2001) 341.
[6] Yu. Chang, A. Ko, Appl. Catal. A 190 (2000) 149.
[7] W. Kagunya, W. Jones, Appl. Clay Sci. 10 (1995) 95.
[8] M.S. Jeong, H. Frei, J. Mol. Catal. A 156 (2000) 245.
[9] L.M. Baigrie, R.A. Cox, H.S. Tilk, M. Teneer, T.T. Tidwell, J. Am. Chem. Soc. 107 (1985) 3640.
[10] E. Dumitriu, V. Hulea, C. Chelaru, C. Catrinescu, D. Tichit, R. Durand, Appl. Catal. 178 (1999) 145.
[11] A.I. Biaglow, J. Sepa, R.J. Gorte, D. White, J. Catal. 151 (1995) 373.
[12] R.P. Young, N. Sheppard, J. Catal. 7 (1967) 223.
[13] H. Idriss, K.S. Kim, M.A. Barteau, J. Catal. 139 (1993) 119.
[14] J.I. Di Cosimo, V.K. Dıez, M. Xu, E. Iglesia, C.R. Apesteguia, J. Catal. 178 (1998) 499.
[15] M. Singh, N. Zhou, D.K. Paul, K.J. Klabunde, J. Catal. 260 (2008) 371.
[16] B.A. Morrow, A.J. McFarlan, J. Phys. Chem. 96 (1992) 1395.
[17] Z. Dang, B.G. Anderson, Y. Amenomiya, B.A. Morrow, J. Phys. Chem. 99 (1995) 14437.
[18] Y. Chen, J. Han, H. Zhang, Appl. Surf. Sci. 254 (2008) 5967.
[19] M.I. Lianos, T. Lopez, R. Gomez, Langmuir 13 (1997) 974.
[20] T. Yamaguchi, T. Morita, T.M. Salama, K. Tanabe, Catal. Lett. 4 (1990) 1.
[21] V.K. Diez, C.R. Apesteguia, J.I. Di Cosimo, Catal. Today 63 (2000) 53.
[22] Z. Wang, H. Wan, B. Liu, X. Zhao, X. Li, H. Zhu, X. Xu, F. Ji, K. Sun, L. Dong, Y. Chen, J. Colloid Interface Sci. 320 (2008) 520.
[23] R. Philipp, K. Fujimoto, J. Phys. Chem. 96 (1992) 9035.
[24] J.V. Evans, T.L. Whateley, Trans. Faraday Soc. 63 (1967) 2769.
[25] J.A. Lercher, C. Colombier, H. Noller, J. Chem. Soc. Faraday Trans. 80 (1984) 949.
[26] W. Hertl, Langmuir 5 (1989) 96.
[27] S.J. Gregg, J.D. Ramsay, J. Chem, Soc. (1970) 2784.
[28] M.C. Kung, H.H. Kung, Catal. Rev. – Sci. Eng. 27 (1985) 425.
[29] B.A. Morrow, I.A. Cody, J. Phys. Chem. 80 (1976) 1995.
[30] J. Nawrocki, M.P. Rigney, A. McCormick, P.W. Carr, J. Chromatogr. 14 (1993) 211.
[31] J.A. Lercher, React. Kinet. Catal. Lett. 20 (1982) 409.
[32] C. Li, G. Li, Q. Xin, J. Phys. Chem. 98 (1994) 1933.
[33] Y.-Ch. Chang, A.-N. Ko, Appl. Catal. A. 190 (2000) 149.
[34] E. Arundale, L.A. Mikeska, Chem. Rev. 51 (3) (1952) 505.
[35] M.J.L. Gines, E. Iglesia, J. Catal. 176 (1998) 155.
[36] H. Idriss, K. Pierce, M.A. Barteau, J. Am. Chem. Soc. 113 (1991) 715.
[37] H. Idriss, C. Diagne, J.P. Hindermann, A. Kiennemann, M.A. Barteau, J. Catal. 155 (1995) 219.
[38] X. Gao, J.L.G. Fierro, I.E. Wachs, Langmuir 15 (1999) 3169.
[39] G. Zhang, H. Hattori, K. Tanabe, Bull. Chem. Soc. Jpn. 62 (1989) 2070.
[40] W. Hill, H. Miessner, G. Öhlmann, J. Chem. Soc. Faraday Trans. 85 (1989) 691.
[41] A.A. Tsyganenko, E.N. Storozheva, O.V. Manoilova, T. Lesage, M. Daturi, J.-C. Lavalley, Catal. Lett. 70 (2000) 159.
[42] R.P. Young, Can. J. Chem. 47 (1969) 2237.
[43] I.R. Subbotina, V.B. Kazansky, F.C. Jentoft, R. Schlögl, Stud. Surf. Sci. Catal. 174 (2008) 849.
[44] A. Gervasini, C. Messi, D. Flahaut, C. Guimon, Appl. Catal. 367 (2009) 113.
[45] Z. Dang, P.B.G. Anderson, Y. Amenomiya, B.A. Morrow, J. Phys. Chem. 99 (1995) 14437.